Dalton Transactions

PAPER

View Article Online
View Journal | View Issue

Cite this: *Dalton Trans.*, 2014, **43**, 568

Structural diversity in hybrid vanadium(IV) oxyfluorides based on a common building block†

Farida H. Aidoudi, Cameron Black, Kasun S. Athukorala Arachchige, Alexandra M. Z. Slawin, Russell E. Morris and Philip Lightfoot*

Received 29th August 2013,
Accepted 4th October 2013

DOI: 10.1039/c3dt52385c

www.rsc.org/dalton

There are only limited reports on vanadium(IV) oxyfluorides (VOFs) with extended crystal structures. Here we expand and enrich the list of existing VOFs with a series of 14 new materials "**VOF-*n***" (*n* = 1–14)" prepared using ionothermal and solvothermal synthesis methods. All of these materials arise from the condensation of a dimeric structural motif. These VOFs can be classified into three groups depending on their key structural features; *layer structures*: **VOF-1** "$[HN_2C_7H_6][V_2O_2F_5]$", **VOF-2** "$[HN_2C_4H_4][V_2O_2F_5]$", **VOF-3** "$[HN_2C_3H_4][V_2O_2F_5]$" and **VOF-4** "$V_2(N_2C_4H_4)O_2F_4$", *ladder like structures*: **VOF-5** "$[NH_4(HN_2C_3H_4)][V_2O_2F_6]$", **VOF-6** "$[K(HN_2C_3H_4)][V_2O_2F_6]$", **VOF-7** "$[HNH_2CH_2CH_3][VOF_3]$", **VOF-8** "$[HN_2C_7H_6][VOF_3]$", **VOF-9** "$[H_2N_2C_4H_6][V_2O_2F_6]$", **VOF-10** "β-$RbVOF_3$", **VOF-11** "α-$KVOF_3$", **VOF-12** "β-$KVOF_3$", **VOF-13** "$[H_2(NH_2)_2(CH_2)_2][V_2O_2F_6]$", and a *chain structure*: **VOF-14** "$[H_2N_2C_6H_{12}][V_2O_2F_7]$". The crystal structures of **VOF-*n*** are presented, and their synthetic and structural relationships are discussed.

Introduction

Compounds of vanadium(IV) exhibiting extended lattice structures are of interest for a variety of properties and applications, for example as lithium battery cathodes,[1] frustrated magnets[2] and oxidation catalysts.[3] We have focused our own interest over the past few years on the synthesis of metal (oxy)fluorides[4] with particular emphasis on developing novel hybrid organic–inorganic vanadium (oxy)fluorides using various synthetic methods, including hydrothermal and ionothermal systems. This has resulted in a wide range of materials containing vanadium in III, IV or V oxidation states.[5–8]

The many variables involved in both hydrothermal and ionothermal systems illustrate their complexity, and in the course of our exploratory studies we have found that the outcomes of these reactions are very sensitive to small changes in conditions. In addition to the vital role of the solvent, many other factors (*e.g.* vanadium source, amount of HF, nature and amount of the added template and others) may affect the reaction outcome. Although the direct impact of these parameters on the resulting materials is not yet fully understood, there is a clear indication of the propensity of ionothermal systems,[9] *i.e.* using ionic liquids (ILs) as the reaction solvent, to produce more extended V(IV)-containing fluorides. For instance hydrothermal synthesis mainly produces low dimensional VOFs; monomeric, oligomeric or chain-type structures are all accessible hydrothermally at low reaction temperatures. On the other hand more extended VOF structures are accessible using ionothermal synthesis, where a hydrophobic IL, 1-ethyl-3-methylimidazolium bis(trifluoromethylsulfonyl)imide (EMIM Tf_2N) is used as the reaction solvent. Initially, this led to the preparation of the first VOF with a 2-D connectivity, [H*pyr*]-$[V_2O_2F_5]$,[10] and subsequently, a similar approach allowed us to prepare a VOF with a pillared-layer kagome lattice, $[NH_4]_2[HNC_7H_{13}][V_7O_6F_{18}]$.[11] Very recent studies demonstrate that this material displays unusual gapless quantum spin-liquid behaviour.[12]

We have pursued further research on both ionothermal and hydrothermal synthesis of VOFs, yielding a variety of further, novel V(IV)-containing materials with a very rich crystal chemistry. All the materials reported herein contain vanadium in the IV oxidation state, and are based on a common dimeric structural motif. The order in which the structures are presented follows their dimensionality, and the structures are given the symbols **VOF-*n***.

Experimental section

Synthesis

All reagents were commercially available and used without further purification, except the ionic liquids EMIM Tf_2N and *N*-butylpyridinium bromide (BPB), which were synthesised according to the literature procedure.[13,14]

EaStChem, School of Chemistry, University of St Andrews, St Andrews, Fife KY16 9ST, UK. E-mail: pl@st-and.ac.uk

†Electronic supplementary information (ESI) available. CCDC 957929–957939. For ESI and crystallographic data in CIF or other electronic format see DOI: 10.1039/c3dt52385c

Among the VOFs presented here, only **VOF-10**, **VOF-11** and **VOF-12** were synthesised solvothermally in a 40 mL Teflon-lined stainless steel autoclave using either a mixture of water–DMSO or water–ethylene glycol. All the other VOFs were made ionothermally in a 30 mL Teflon-lined stainless steel autoclave.

All the ionothermally prepared VOFs were synthesised following a typical synthesis procedure: a Teflon-lined autoclave (volume 30 mL) was charged with VOF_3 (0.124 g, 1 mmol, Sigma Aldrich) (or V_2O_5 (0.182 g, 1 mmol, Sigma Aldrich) in the case of **VOF-13**) and HF (48 wt% in H_2O) (0.1 mL, 2.76 mmol, Sigma Aldrich) or (1 mL, 27.6 mmol, Sigma Aldrich in the case of **VOF-13**) and then the IL EMIM Tf_2N (4 g, ~10 mmol) (or the IL EPB 2.16 g, ~10 mmol in the case of **VOF-13**) was added along with the added template; benzimidazole (**VOF-1** and **VOF-8**), pyrazine (**VOF-2** and **VOF-4**), imidazole (**VOF-3** and **VOF-5**), imidazole and KNO_3 (**VOF-6**), ethylamine (**VOF-7**), 2-methylimidazole (**VOF-9**), ethylenediamine (**VOF-13**) and 1,4-diazabicyclo[2.2.2]octane (DABCO) (**VOF-14**).

For **VOF-1**, **VOF-2**, **VOF-3**, **VOF-5**, **VOF-6**, **VOF-7**, **VOF-8** and **VOF-9** the stainless steel autoclave was then sealed and heated in an oven at 170 °C for 24 h; for **VOF-4** and **VOF-13** the autoclave was heated at 140 °C for 24 h and for **VOF-14** the autoclave was heated at 130 °C for 24 h. After the autoclave had been cooled to room temperature, the product was filtered, washed with methanol and dried in air for 24 h.

A general scheme for the synthesis of **VOF-10**, **VOF-11** and **VOF-12** solvothermally is as follows: a Teflon-lined autoclave (volume 40 mL) was charged with V_2O_5 (0.182 g, 1 mmol, Sigma Aldrich) and RbF (0.209 g, 2 mmol) or K_2CO_3 (0.136 g, 1 mmol) and HF (48 wt% in H_2O) (0.5 mL, 13.8 mmol, Sigma Aldrich). and then a solution of 3 : 1 H_2O–DMSO, 4 : 5 H_2O–ethylene glycol or 7 : 1 H_2O–ethylene glycol was added respectively. The stainless steel autoclave was then sealed and heated in an oven at 160 °C for 24 h or 72 h.

The synthesis procedure for the ILs and for each compound can be found in full detail in the ESI.†

X-ray crystallography

Single crystal X-ray diffraction data for **VOF-1** were collected at station 11.3.1 of the Advanced Light Source at Lawrence Berkeley National Laboratories, California using a Bruker APEX II CCD diffractometer. Single crystal X-ray diffraction data for all other VOFs were collected using Mo-Kα (0.7107 Å) radiation utilising a Rigaku rotating anode single-crystal X-ray diffractometer at the University of St Andrews. The structures were solved with standard direct methods using SHELXS and refined with least-squares minimisation techniques against F^2 using SHELXL within the WinGX packages.

Powder XRD was carried out on a Stoe STADI/P diffractometer using Cu $K_{\alpha 1}$ X-rays.

VOF-3 displays an inorganic layer that shows an interesting variation to the one previously seen in [H*pyr*][$V_2O_2F_5$].[10] **VOF-4**, **VOF-13** and **VOF-14** display novel polyhedral connectivities that are unprecedented in this class of materials. For space reasons only the crystallographic details for these materials are presented in Table 1; for all the other structures they are tabulated in the ESI.†

Magnetic measurements

Magnetic susceptibility data for **VOF-13** were collected on a Quantum Design MPMS SQUID. Data were recorded in a 2000 Oe field while warming the sample from 1.8 to 300 K in 4 K steps, following consecutive zero-field cooling (ZFC) and field cooling (FC) cycles. Data were normalized to the molar quantity of the sample, and corrected for any diamagnetic contributions.

Table 1 Crystallographic data for **VOF-3**, **VOF-4**, **VOF-13** and **VOF-14**

	VOF-3	VOF-4	VOF-13	VOF-14
Formula	$[HC_3N_2H_4][V_2O_2F_5]$	$V_2(N_2C_4H_4)O_2F_4$	$[H_2(NH_2)_2(CH_2)_2][V_2O_2F_6]$	$[H_2N_2C_6H_{12}][V_2O_2F_7]$
Fw/g mol^{-1}	297.97	289.97	310	381.07
Space group	$P2_1$ (4)	$P2_1/c$ (14)	$P2_1/m$ (11)	$C2/c$ (15)
a/Å	7.170(3)	5.0096(14)	8.806(3)	10.0330(19)
b/Å	17.333(7)	10.8260(3)	12.100(5)	10.0380(17)
c/Å	7.370(4)	7.288(7)	9.206(4)	11.930(2)
α/°	90	90	90	90
β/°	118.0531(10)	95.9430(10)	106.301(2)	110.170(3)
γ/°	90	90	90	90
V/Å^3	808.32(6)	393.1(4)	941.49(6)	1127.8(3)
Z	4	2	4	4
Crystal size/mm	0.25 × 0.03 × 0.02	0.20 × 0.20 × 0.12	0.2 × 0.2 × 0.2	0.05 × 0.05 × 0.05
Crystal shape and colour	Blue needle	Blue platelet	Blue prism	Blue prism
F(000)	576	280	608	680
R_{int}	0.0509	0.0247	0.0601	0.1031
Obsd data [$I > 2\sigma(I)$]	1875	612	1711	891
Data/restraints/parameters	2153/1/254	710/0/72	1821/0/125	1046/0/96
GOOF on F^2	1.013	1.069	1.241	1.019
R_1, wR_2 ($I > 2\sigma(I)$)	0.0395, 0.0772	0.0262, 0.0540	0.1123, 0.2515	0.0871, 0.2332
R_1, wR_2 (all data)	0.0468, 0.0815	0.0337, 0.0565	0.1180, 0.2551	0.0970, 0.2486
Largest diff. peak/hole	0.522/−0.504	0.318/−0.368	2.314/−1.787	1.775/−0.847

Results and discussion

Crystal structures

The VOF structures presented here fall into three major groups: 2-D layers, 1-D ladder-like chains and a 1-D single chain.

Interestingly all these structures can be regarded as arising from the same structural motif, where in all the structures the coordination environment around each vanadium atom is highly distorted (typical characteristic of V(IV) in vanadium oxyfluorides) due to the presence of the short vanadyl V=O bond (~1.6 Å) and the corresponding elongated *trans* V–F bond (~2.2 Å); the other V–F bonds are within the normal range (~1.9 Å).[7]

The vanadyl group is terminal in all the structures, with an additional common feature being two F atoms bridging two adjacent octahedral units into an edge-shared dimer. These dimers, are then further linked to others in different ways to form layers, ladders or chains. The dimer in **VOF-4** is slightly different with the vanadyl group being *cis*- rather than *trans*- to the bridging F atoms, and two N atoms from the pyrazine ligand taking up one of the *trans*-positions (V–N distance 2.121(3) Å). These two types of edge-shared-dimers are shown in Fig. 1.‡

VOF-1 and **VOF-2** arise from the condensation of the edge-shared dimers, described earlier, through bridging F-atoms to form infinite "ladder" like chains (Fig. 2). These chains are further linked through F atoms leaving only O atoms terminal, to form an infinite anionic layer of composition $[V_2O_2F_5]_n^{n-}$ (Fig. 3), similar to the one previously seen in [H*pyr*][$V_2O_2F_5$].[10] These layers are separated *via* hydrogen-bonded protonated organic amine moieties, benzimidazolium, or pyrazinium (Fig. 4).

In **VOF-1** there are four vanadium ions in the asymmetric unit, and in **VOF-2** there are two vanadium ions in the asymmetric unit, all of which are in the 4+ oxidation state as confirmed by bond valence sum calculations (see ESI†).

VOF-3 is also constructed from the edge-shared dimer described earlier, with the dimers sharing F atoms to form infinite "ladder" like chains in a similar way as **VOF-1** and

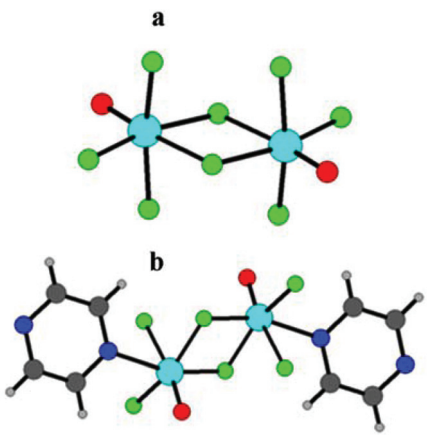

Fig. 1 The dimeric $[V_2O_2F_8]^{4-}$ building units observed in (a) all the **VOF-*n*** structures except **VOF-4** and (b) dimeric unit observed in **VOF-4**.

‡Colour scheme used in all pictures: vanadium (light blue), fluorine (green), oxygen (red), nitrogen (dark blue), carbon (dark grey), hydrogen (light grey), potassium (pink) and rubidium (purple).

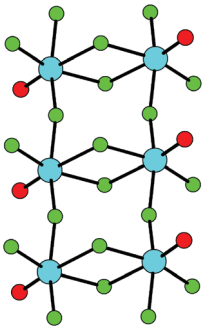

Fig. 2 Ladder type $[VOF_3]_n^{n-}$ chain.

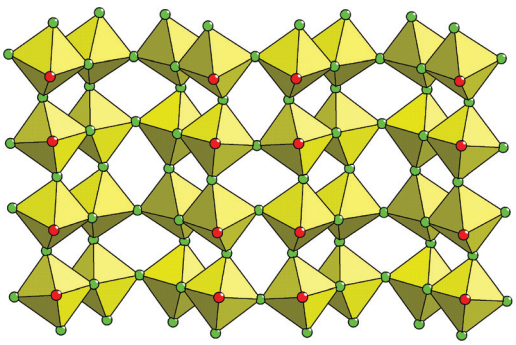

Fig. 3 $[V_2O_2F_5]_n^{n-}$ layer found in **VOF-1** and **VOF-2**.

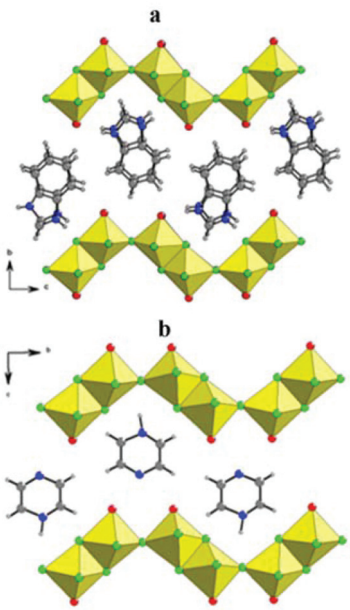

Fig. 4 A view of the layer packing in (a) **VOF-1** and (b) **VOF-2**.

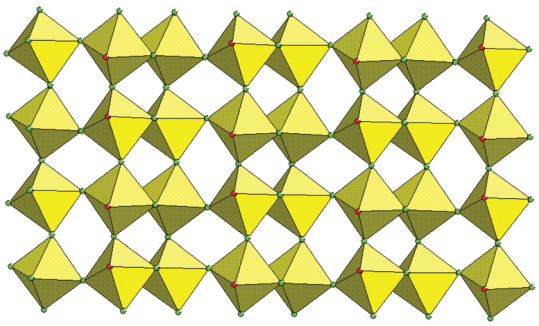

Fig. 5 $[V_2O_2F_5]_n^{n-}$ layer found in **VOF-3**.

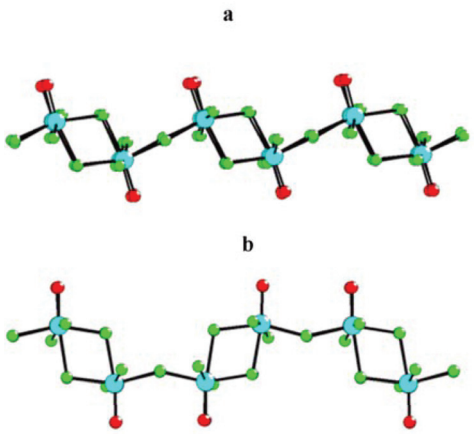

Fig. 6 A view of the polymorphic **3** $[V_2O_2F_5]_n^{n-}$ layers: (a) found in **VOF-3** (b) found in **VOF-1** and **VOF-2**.

VOF-2. These chains are then joined through F atoms to form an infinite anionic layer (Fig. 5). Interestingly, as shown in Fig. 6, the ladders in **VOF-3** are linked in a different way compared to **VOF-1** and **VOF-2**. In **VOF-3** the nearest "vanadyl" bonds from two adjacent ladders point in opposite directions (Fig. 6(a)); in contrast, in **VOF-1** and **VOF-2** they point in the same direction (Fig. 6(b)).

In **VOF-3** the layers are separated *via* hydrogen-bonded protonated imidazolium cations (Fig. 7).

It can be seen that the arrangement of the ladders within two different layers in **VOF-1** and **VOF-2** follow the same pattern previously seen in [H*pyr*][$V_2O_2F_5$]: *i.e.* corrugated layers arranged parallel to each other while in **VOF-3** they are quite different, and are aligned in nearly anti-parallel fashion.

VOF-4 displays a 2-D coordination polymer motif, built up from the edge-sharing dimer described earlier (Fig. 1(b)), which is further linked to other adjacent dimers through two bridging F-atoms to form an edge-sharing "zigzag" chain (Fig. 8). These chains are bridged by the pyrazine ligand to form infinite metal–organic sheets (Fig. 9 and 10).

In **VOF-4** there is only one single vanadium ion in the 4+ oxidation state as confirmed by bond valence sum calculations ($\sum V_1 = 3.77$).

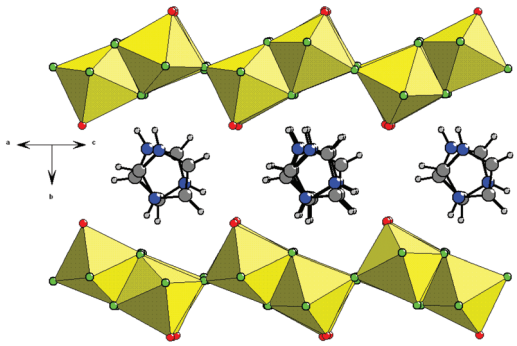

Fig. 7 A view of the layer packing in **VOF-3**.

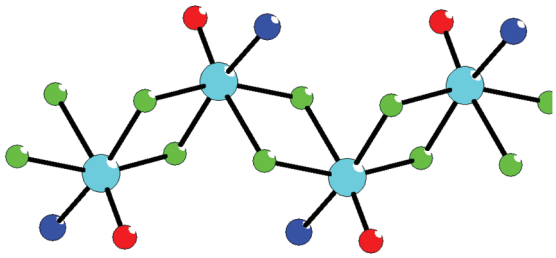

Fig. 8 Inorganic chain found in **VOF-4**.

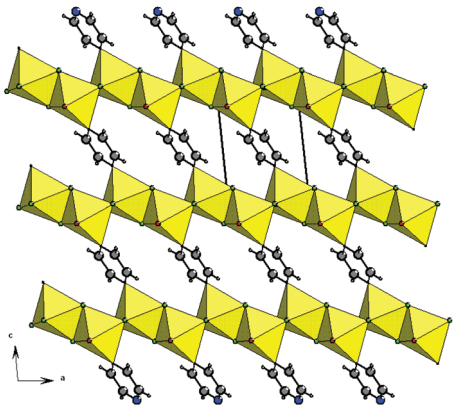

Fig. 9 The V(IV) oxyfluoride/pyrazine layer found in **VOF-4**.

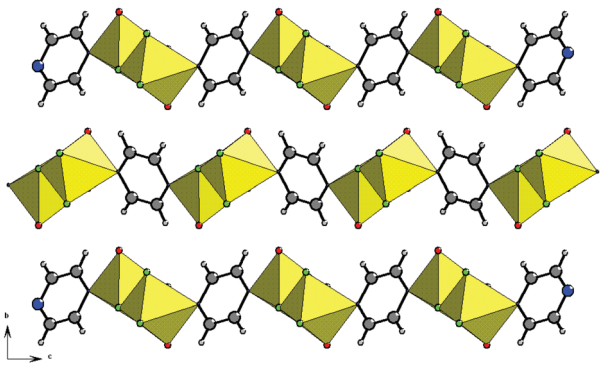

Fig. 10 Structure of **VOF-4** viewed along the *a* axis, showing stacks of layers.

Edge-sharing octahedral chains bridged by organic ligands have previously been reported for divalent metal chlorides bridged by *bipy*[15–17] and *trans*-connected single chains have also been seen in vanadium and magnesium fluorides bridged by *bipy*,[6,18] but there are no previous reports on "zigzag" edge-sharing chains in metal-halide/organic coordination polymers.

VOF-4 was synthesised using the same procedure as **VOF-2**, the only difference being the reaction temperature (140 °C for **VOF-4** and 170 °C for **VOF-2**). It is interesting to see how the reaction temperature affects the resulting materials and also the protonation of the organic amine involved within the synthesis.

High temperature reaction conditions led to more condensation of the inorganic framework to form 2-D anionic inorganic sheets templated by protonated pyrazinium cations, whereas lower reaction temperatures did not favour either increased condensation of the inorganic framework or the protonation of pyrazine, and hence a 2-D coordination polymer was formed.

VOF-5, **VOF-6**, **VOF-7**, **VOF-8**, **VOF-9**, **VOF-10**, **VOF-11** and **VOF-12** all display the same inorganic ladder-type chain previously reported for $CsVOF_3$, α-$RbVOF_3$ and $[H_2bpe]_{1/2}VOF_3$.[19] This ladder (Fig. 2) is constructed from the edge-sharing dimer described earlier (see Fig. 1(a)), with each dimer sharing two further F atoms with adjacent dimers, leaving one F and one O atom terminal.

All the ladder type materials contain one single vanadium site in the asymmetric unit, with bond valence sum calculations indicating a 4+ oxidation state in each case.

Interestingly, this type of vanadium octahedral connectivity can be achieved using organic, inorganic or mixed organic–inorganic templates, and is produced using either solvothermal or ionothermal synthesis.

While the ladder-like motif always displays essentially the same structural features (*i.e.* distribution of bond lengths and the orientation of the vanadyl bond), the different templates involved in the synthesis dictate different overall crystal-packing characteristics. In fact, it is not only the template that affects the overall structural features: a subtle change in the reaction conditions can give rise to different polymorphs of the same composition. For example, prior to our synthesis of **VOF-10** a different modification (now designated α-$RbVOF_3$) had been reported[19] and was synthesised using a solution of 1 : 1 H_2O–ethylene glycol. Changing the mixed solvent system to 3 : 1 H_2O–DMSO led to the second polymorph (**VOF-10**, or β-$RbVOF_3$) with a different ladder packing scheme. Also **VOF-11** and **VOF-12**, polymorphs of $KVOF_3$, can both be synthesised by varying the ratio of the mixed solvent system and the temperature.

The crystal packing schemes for **VOF-5**, **VOF-6**, **VOF-7**, **VOF-8**, **VOF-9**, **VOF-10**, **VOF-11** and **VOF-12** are shown in Fig. 11–13.

It is worth mentioning, here, that the layer structure **VOF-1** and the ladder **VOF-8** have been prepared using the same template benzimidazole; using 1 mmol led to **VOF-1** as a pure phase, slightly increasing this amount to 1.5 mmol led to a

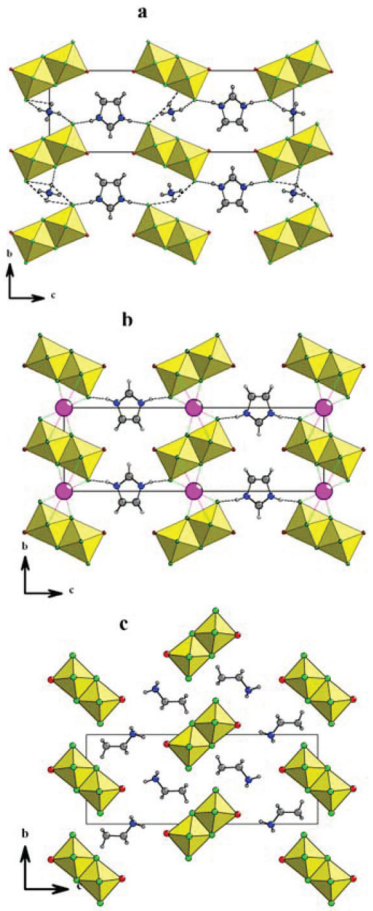

Fig. 11 Structure of **VOF-5** (a), **VOF-6** (b) and **VOF-7** (c) viewed along the *a* axis.

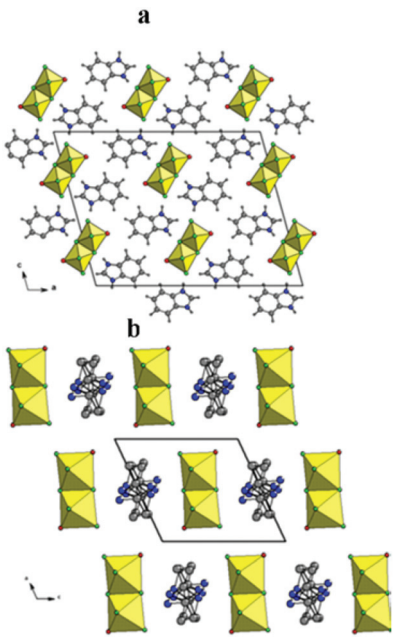

Fig. 12 Structures of **VOF-8** (a) and **VOF-9** (b) viewed along the *b* axis.

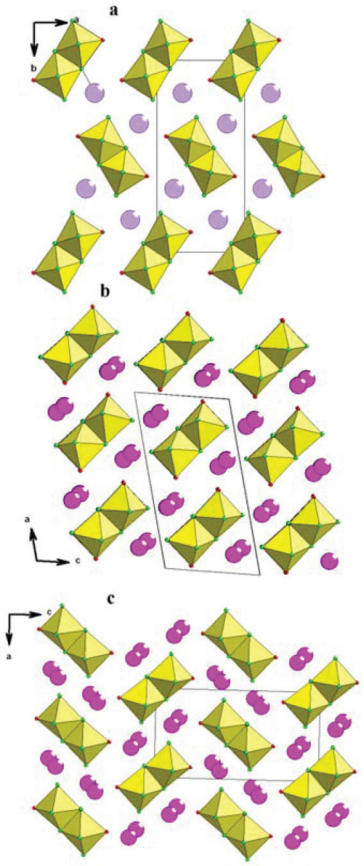

Fig. 13 Structures of **VOF-10** (a) viewed along the *c* axis, **VOF-11** (b) and **VOF-12** (c) viewed along the *b* axis.

sample containing mixed phases of **VOF-1** and **VOF-8**. The layered structure **VOF-3** also coexists with the ladder type structure **VOF-5**, and several attempts to prepare them phase-pure were not successful (see ESI† for more details on the synthesis conditions and also PXRDs for the samples).

The crystal structure of **VOF-13** shows an interesting variation of the 'standard' $[VOF_3]_n^{n-}$ ladder-type described above. In the standard ladder, the edge-sharing dimer can be considered as the *rung* of the ladder, with each octahedral unit of the dimer further sharing one F atom with adjacent octahedra to form the *rails* (Fig. 2). In contrast, **VOF-13** can be regarded as an "alternating ladder-type structure" where the edge-sharing dimer is not the *rung* of the ladder but instead forms part of the *rails*; the *rung* is the tetrameric unit formed when the dimers share two further F atoms, and these tetrameric units are linked to each other by sharing two more F atoms (Fig. 14). Fig. 15 shows the "buckled" nature of the "alternating" ladder compared to the "standard" ladder.

It can also be seen that both types of ladders, the 'standard' and the 'alternating' one may be regarded as constituent motifs of the layers found in **VOF-1** and **VOF-2** (see Fig. S11 in the ESI†) where the "standard ladder" can be seen in the vertical direction, while the "alternating ladder" appears in the horizontal direction.

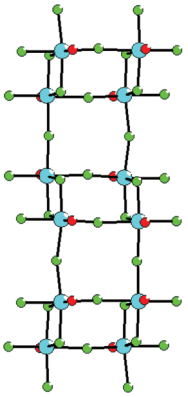

Fig. 14 Topology of the $[VOF_3]_n^{n-}$ "alternating ladder" chain.

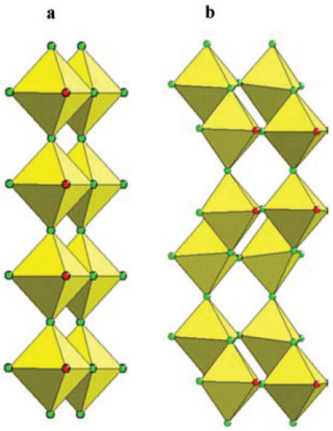

Fig. 15 A view showing the standard ladder (a) and the alternating ladder (b).

In **VOF-13**, the ladders are linked together by protonated ethylenediammonium cations as illustrated in Fig. 16.

VOF-14 has a novel chain type structure. Again, this chain, as illustrated in Fig. 17, is formed from the edge-sharing dimers described earlier, with each dimeric unit sharing only one further F atom with neighbouring units, leaving two F atoms and one O atom terminal. The chains are connected

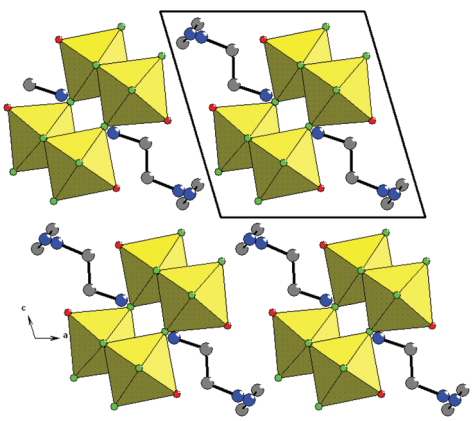

Fig. 16 **VOF-13** viewed along the *b* axis.

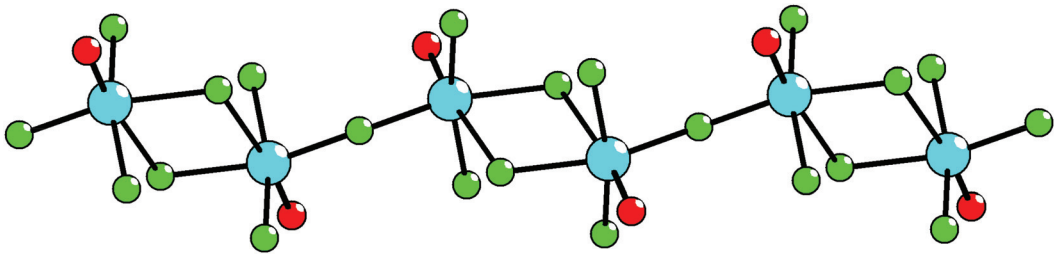

Fig. 17 Unique chain type $[V_2O_2F_7]_n^{2n-}$ motif found in **VOF-14**.

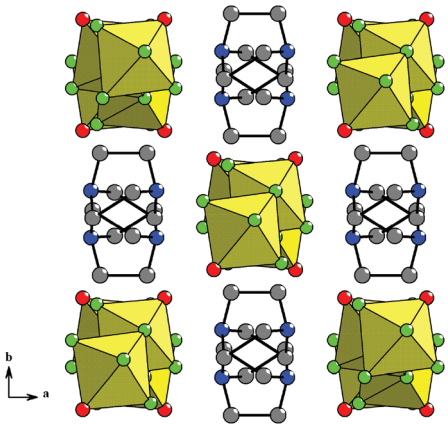

Fig. 18 A view of **VOF-14** along the *c* axis.

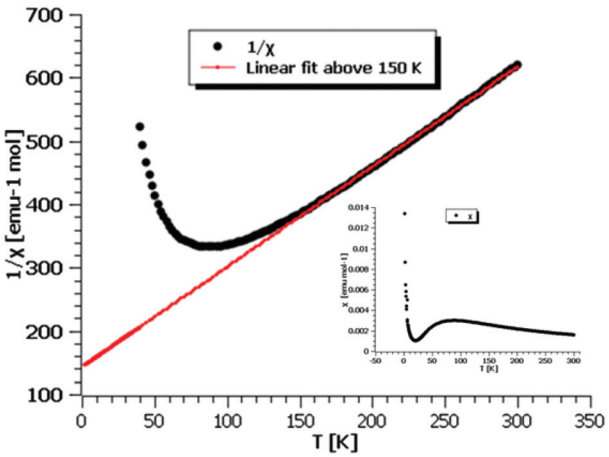

Fig. 19 Plot of $1/\chi$ *versus* *T* and the Curie–Weiss fit above 150 K for **VOF-13**; the inset shows the plot of χ *versus* *T*.

through protonated DABCO cations as shown in Fig. 18. It is worth noting that according to the bond valence sum calculations, ($\sum V_1$ = 4.77) and also looking at the formula (with only one H_2DABCO), vanadium occurs in a mixed +4/+5 oxidation states.

Magnetic susceptibility

As shown in Fig. 19, magnetic susceptibility data for **VOF-13** show evidence for low-dimensional antiferromagnetic order, with a broad maximum in the plot of χ *versus* *T* near 50 K (see the inset in Fig. 19). Above 150 K the data fit well to a Curie–Weiss law, with a Weiss constant $\theta = -90$ K indicating relatively strong antiferromagnetic interactions. The experimental effective magnetic moment $\mu_{eff} = 2.29\mu_B$ is in good agreement with the ideal value for two isolated spin 1/2 species (*i.e.* two V(IV) per formula unit), $\mu_{ideal} = 2.45\mu_B$.

Various simple models were used to attempt to fit the $\chi(T)$ data, including Bleaney–Bowers dimer, 1D Ising or Heisenberg chains and spin ladder models. The best fit was produced from a 1-D $S = 1/2$ Ising chain model (see ESI†), rather than the Heisenberg chain (in contrast to the ladder compound $CsVOF_3$).[19]

Conclusions

The reaction of VOF_3 or V_2O_5, HF and an appropriate organic, inorganic or mixed templating source in a suitable solvent (IL or a solution of H_2O–DMSO or H_2O–ethylene glycol) yielded 14 novel materials, that considerably expand and enrich the list of existing VOFs. Both ionothermal and solvothermal systems are shown to be fruitful media to target these types of materials. These results emphasise once more the propensity of ionothermal synthesis to produce more extended structures, with the isolation of four novel materials displaying 2-D connectivities, although ladder type structures and 1-D chains are still accessible ionothermally. In ionothermal synthesis using a hydrophobic IL, EMIM Tf_2N, the nature and the amount of the templating source involved in the synthesis has a great effect on the dimensionality of the final material. The reaction temperature can also affect the degree of protonation of template. High reaction temperature leads to the protonation of pyrazine and the formation of a 2-D inorganic layer with the pyrazinium cations acting as a template and charge balancing agent (**VOF-2**), while lower temperature yielded a neutral layered coordination polymer with pyrazine acting as a coordinating ligand (**VOF-4**). Solvothermal synthesis yielded three different phases displaying ladder like topologies and it is found that a subtle change in the reaction conditions affects the conformation of the ladders and their packing within the unit cell (**VOF-10**, **VOF-11**, **VOF-12**). While this exploration yielded several interesting materials, it is apparent that there is still much more scope to develop further the chemistry of

VOFs, leading to other new VOF framework types and potentially novel physical or chemical properties.

Acknowledgements

We thank Dr Phoebe K. Allan and Dr Catherine Renouf for assistance in collecting diffraction data for VOF-1 and Mr Lewis J. Downie for assistance in collecting the magnetic data. We thank the EPSRC for funding under grant numbers EP/F021925 and EP/K005499/1. FHA also acknowledges support from the EPSRC Doctoral Prize Fellowships scheme (EP/J500549/1).

Notes and references

1 J. Song, M. Xu, L. Wang and J. B. Goodenough, *Chem. Commun.*, 2013, **49**, 5280.
2 A. A. Tsirlin and H. Rosner, *Phys. Rev. B: Condens. Matter*, 2009, **79**, 214417.
3 M. Eichelbaum, M. Hävecker, C. Heine, A. Karpov, C.-K. Dobner, F. Rosowski, A. Trunschke and R. Schlögl, *Angew. Chem., Int. Ed.*, 2012, **51**, 6246.
4 K. Adil, M. Leblanc, V. Maisonneuve and P. Lightfoot, *Dalton Trans.*, 2010, **39**, 5983.
5 T. Mahenthirarajah, Y. Li and P. Lightfoot, *Inorg. Chem.*, 2008, **47**, 9097.
6 D. W. Aldous, N. F. Stephens and P. Lightfoot, *Inorg. Chem.*, 2007, **46**, 3996.
7 D. W. Aldous, N. F. Stephens and P. Lightfoot, *Dalton Trans.*, 2007, 2271.
8 D. W. Aldous, N. F. Stephens and P. Lightfoot, *Dalton Trans.*, 2007, 4207.
9 R. E. Morris, *Chem. Commun.*, 2009, 2990.
10 F. Himeur, P. K. Allan, S. J. Teat, R. J. Goff, R. E. Morris and P. Lightfoot, *Dalton Trans.*, 2010, **39**, 6018.
11 F. H. Aidoudi, D. W. Aldous, R. J. Goff, A. M. Z. Slawin, J. P. Attfield, R. E. Morris and P. Lightfoot, *Nat. Chem.*, 2011, **3**, 801.
12 L. Clark, J. C. Orain, F. Bert, M. A. De Vries, F. H. Aidoudi, R. E. Morris, P. Lightfoot, J. S. Lord, M. T. F. Telling, P. Bonville, J. P. Attfield, P. Mendels and A. Harrison, *Phys. Rev. Lett.*, 2013, **110**, 207208.
13 P. Harrison, A.-P. Dias, N. Papageorgiou, K. Kalyanasundaram and M. Gratzel, *Inorg. Chem.*, 1996, **35**, 1168.
14 G. S. Owens and M. M. Abu-Omar, *J. Mol. Catal. A: Chem.*, 2002, **187**, 215.
15 M. A. Lawandy, X. Huang, R.-J. Wang, J. Li, J. Y. Lu, T. Yuen and C. L. Lin, *Inorg. Chem.*, 1999, **38**, 5410.
16 C. Hu and U. Englert, *Angew. Chem., Int. Ed.*, 2005, **44**, 2281.
17 A. M. Chippindale, A. R. Cowley and K. J. Peacock, *Acta Crystallogr., Sect. C: Cryst. Struct. Commun.*, 2000, **56**, 651.
18 J. Darriet, W. Massa, J. Pebler and R. Stief, *Solid State Sci.*, 2002, **4**, 1499.
19 D. W. Aldous, R. J. Goff, J. P. Attfield and P. Lightfoot, *Inorg. Chem.*, 2007, **46**, 1277.